INTERNATIONAL JOURNAL FOR NUMERICAL METHODS IN FLUIDS, VOL. 14, 907–918 (1992)

A PREDICTION OF THE PRESSURE FIELD IN A PLANE TURBULENT JET USING AN ALGEBRAIC STRESS MODEL

DONALD J. BERGSTROM

Department of Mechanical Engineering, University of Saskatchewan, Saskatoon, Saskatchewan, Canada S7N 0W0

SUMMARY

A numerical prediction is obtained for the mean pressure field in the similarity region of a plane turbulent jet. An algebraic stress model, which introduces non-isotropic relations for the Reynolds stress components, is used to close the mean momentum equation. The full two-dimensional form of the transport equations is retained and the resultant equation set solved elliptically. The numerical prediction simulates many of the characteristics of the pressure field measured by experimental studies. However, the overall level of the predicted field is lower than the experimental values. The level obtained for the mean pressure field depends strongly on the prediction for the transverse normal Reynolds stress component $\langle u_2 u_2 \rangle$. The pressure field is shown to represent a small negative contribution to the net streamwise momentum balance.

KEY WORDS Elliptic solution Mean pressure Plane turbulent jet Algebraic stress model

1. INTRODUCTION

Turbulent jets represent a class of free shear flows with important industrial and environmental applications. Jets have also been used as 'benchmark' flows for evaluating turbulence models.

In computational studies of jets the usual approach is to approximate the flow as a 'boundary layer' which may then be treated by a parabolic solution technique. Classical boundary layer flows are characterized by the fact that the transverse velocity is relatively small compared to the streamwise component; the flow itself is usually regarded as being relatively thin. Use of these assumptions in the transverse momentum balance then implies that the pressure gradient in the cross-stream direction is negligible. Thus the static pressure in the flow at any streamwise section is constant and equal to that in the external flow. For jets discharged into a quiescent ambient field the pressure gradient term used in the boundary layer equations is zero.

In some ways a plane turbulent jet is different from the typical boundary layer flow envisaged above. For one thing a turbulent jet is not thin, at least in the sense of a flat plate boundary layer. Furthermore, at the edge of a plane jet the transverse velocity component, i.e. the entrainment velocity, is much larger than the streamwise velocity component, which goes to zero. Unlike an axisymmetric jet, a plane jet creates a non-zero entrainment flow pattern in the surrounding fluid.

The fact that a jet is turbulent also has important implications for the mean pressure field. In a laminar jet the viscous contribution to the normal stress components is relatively small. However, for a turbulent jet the normal Reynolds stress components are of the same order of magnitude as the variation in mean pressure due to the flow. Previous studies have noted that the mean pressure field is closely related to the level of the Reynolds stress components.

Given the above, it is of interest to investigate numerically the mean pressure distribution in a free turbulent shear flow such as the plane jet. Towards this end the present paper considers

0271–2091/92/080907–12$06.00

Received November 1990
Revised July 1991

a computational prediction for the pressure distribution in the similarity region of a plane turbulent jet discharged into uniform and initially quiescent surroundings.

Knowledge of the mean static pressure distribution in a turbulent jet leads to a more precise understanding of the overall momentum balance. The classical theory of a turbulent jet[1] begins with the principle of conservation of the streamwise momentum flux. However, Ramaprian and Chandrasekhara[2] point out that for plane turbulent jets the ratio of the streamwise momentum flux to the initial value at the discharge plane varies significantly from experiment to experiment. Part of the variation may be accounted for by neglect of the contribution of the mean pressure to the streamwise balance. As it turns out, based on the computational study presented below, pressure accounts for approximately 7% of the streamwise momentum balance in a plane turbulent jet.

Probably a more important factor in resolving the variation between different experimental studies is the different far-field boundary conditions associated with each specific experiment.[3] A clear understanding of the role of the pressure in the jet is helpful in determining the effect of different external flow conditions on jet flows.

Most previous computational studies of jets, for example that of Hossain and Rodi,[4] solved the boundary layer form of the equations parabolically. In contrast, the present study retained the full two-dimensional form of the transport equations and solved them elliptically. This approach enabled a numerical prediction for the mean pressure field to be obtained.

The mean momentum equation was closed using an algebraic model for the Reynolds stress. Unlike a k–ε model closure, the algebraic stress model introduced non-isotropic models for the normal Reynolds stress components. Since the level of the mean pressure field is closely related to the level of the Reynolds stress components, the algebraic stress model would be expected to yield a more realistic prediction for the mean pressure field than an isotropic eddy viscosity model.

Only a limited number of experimental[5–7] measurements are available for the mean pressure field in a plane turbulent jet. This is due in part to the difficulty of accurately measuring the pressure field in a free turbulent shear flow. One additional study[8] measured the pressure field in a turbulent rectangular jet. However, in the far field this flow more closely resembles an axisymmetric jet. To the author's knowledge, no numerical prediction has yet been published for the pressure field in a plane turbulent jet.

The remainder of the paper first briefly describes the mathematical model and numerical method. The computational results are then compared with the measurements of Hussain and Clark,[7] the most recent and most comprehensive experimental study available. The prediction for the mean pressure field using the algebraic stress model is found to reproduce most of the essential features of the experimental data, although the level of the predicted field is generally lower than the measured data.

2. MATHEMATICAL MODEL

The mathematical model was based on the mean conservation equations for mass and momentum in a turbulent incompressible flow, i.e.

$$U_{i,i}=0, \tag{1}$$

$$\partial U_i/\partial t + U_j U_{i,j} = -(1/\rho)P_{,i} + (\nu U_{i,j})_{,j} - \langle u_i u_j \rangle_{,j}, \tag{2}$$

where uppercase and lowercase letters denote mean and fluctuating components respectively. In the equations above U_i is the mean velocity and P is the hydrodynamic component of the mean pressure field. In the Cartesian tensor notation adopted, '$,j$' is used to denote partial differentiation with respect to 'x_j'; repeated indices are summed over all possible values, $j=1, 2, 3$.

In order to close the mean momentum equation, a turbulence model relation was required for the Reynolds stress $\langle u_i u_j \rangle$. In the present study the algebraic stress model of Gibson and Launder[9] was adopted. The algebraic model was obtained from the Reynolds stress transport equation by approximating the net convection and diffusion of $\langle u_i u_j \rangle$ using the corresponding terms in the transport equation for the turbulence kinetic energy k. The final form of the expression was as follows:

$$\langle u_i u_j \rangle = \phi(k/\varepsilon)(1-c_2)(P_{ij} - \tfrac{2}{3}\delta_{ij}P_K) + \tfrac{2}{3}\delta_{ij}k, \tag{3}$$

where

$$\phi = (P_K/\varepsilon - 1 + c_1)^{-1}. \tag{4}$$

The expressions

$$P_{ij} = -\langle u_i u_k \rangle U_{j,k} - \langle u_j u_k \rangle U_{i,k} \tag{5}$$

and

$$P_K = -\langle u_i u_j \rangle U_{i,j} \tag{6}$$

are the shear production terms in the transport equations for the Reynolds stress and turbulence kinetic energy respectively.

The final closed equation set also involved transport equations for the turbulence kinetic energy k and its dissipation rate ε. The modelled form of the equations was as follows:

$$\partial k/\partial t + U_j k_{,j} = [(\nu_t/\sigma_K)k_{,j}]_{,j} - \langle u_i u_j \rangle U_{i,j} - \varepsilon, \tag{7}$$

$$\partial \varepsilon/\partial t + U_j \varepsilon_{,j} = [(\nu_t/\sigma_\varepsilon)\varepsilon_{,j}]_{,j} + C_{\varepsilon 1}(1/\tau_M)P_K - C_{\varepsilon 2}(1/\tau_M)\varepsilon, \tag{8}$$

where the turbulence time scale was given by $\tau_M = k/\varepsilon$ (where $_M$ stands for mechanical). In each case the diffusion term was modelled using a transport coefficient based on the turbulent viscosity $\nu_t = C_\mu k^2/\varepsilon$ and an effective turbulent Prandtl number, either σ_K or σ_ε.

For the two-dimensional plane flow considered, the final equation set consisted of the continuity equation, four transport equations for U_1, U_2, k and ε, and three algebraic relations for $\langle u_1 u_1 \rangle$, $\langle u_2 u_2 \rangle$ and $\langle u_1 u_2 \rangle$. The values of the seven empirical constants used in the mathematical model are given in Table I.

3. SOLUTION METHOD

The mathematical equation set was solved numerically for the specific case of a plane turbulent jet. Most other studies, with the exception of Sini and Dekeyser[10] and Haroutunian and Launder,[11] first introduced boundary layer approximations and then solved the conservation equations parabolically. In contrast, the present study retained the full two-dimensional form of the equations and solved them elliptically. This approach enabled a prediction to be obtained for the mean pressure field.

Table I. Turbulence model coefficients

c_μ	σ_K	σ_ε	$c_{\varepsilon 1}$	$c_{\varepsilon 2}$	c_1	c_2
0·09	1·0	1·3	1·44	1·92	2·2	0·55

The solution method followed the finite volume formulation of Raithby *et al.*[12] The equations were first discretized over a two-dimensional orthogonal curvilinear grid. A staggered grid configuration was used to prevent oscillations in the pressure field. The approximation of advected quantities at control volume faces used the weighted upwind profiles suggested by Raithby *et al.* The discrete equations adopted an implicit formulation and retained the transient terms for computational purposes. In the iterative solution technique adopted, the mean velocity and pressure field were solved using the SIMPLEC algorithm. The solution process was terminated when the normalized residuals (per control volume) has been reduced to 10^{-6} or less.

Implementation of the turbulence model equations required special attention. The Reynolds stress components were incorporated into the mean momentum equations using the so-called 'stress–flux' formulation.[12] The effective turbulent diffusion was included in the mean momentum equations using eddy viscosity model relations, while the actual Reynolds stress component less the eddy viscosity contribution was 'lagged' in the source term. The most important advantage of such a numerical formulation is that it facilitates the use of the solution algorithms developed for laminar flow.

The turbulence model equations for the Reynolds stress were embedded within the transport equation set in the following manner. For a given mean velocity field the transport equations for k and ε were solved. The coupling of the equations to each other and to the algebraic stress model relations was based on the use of a constant turbulence time scale $\tau_M = k/\varepsilon$ for each iteration of the turbulence model. For given mean velocity gradients and turbulence time scale, discrete approximations to the algebraic equations were then solved iteratively in an efficient manner. Further details of this aspect of the numerical formulation are presented by Bergstrom *et al.*[13]

A schematic diagram of a plane turbulent jet is given in Figure 1. The Cartesian co-ordinate axes x_1 and x_2 represent the streamwise and transverse flow directions respectively. The jet is assumed to be discharged from a long narrow slot in a flat wall. At the wall the velocity components are assumed to be zero. The outer edge of the solution domain is located sufficiently far away from the centreline for the mean streamwise velocity to be zero. From symmetry it was only necessary to model the half-plane of the jet.

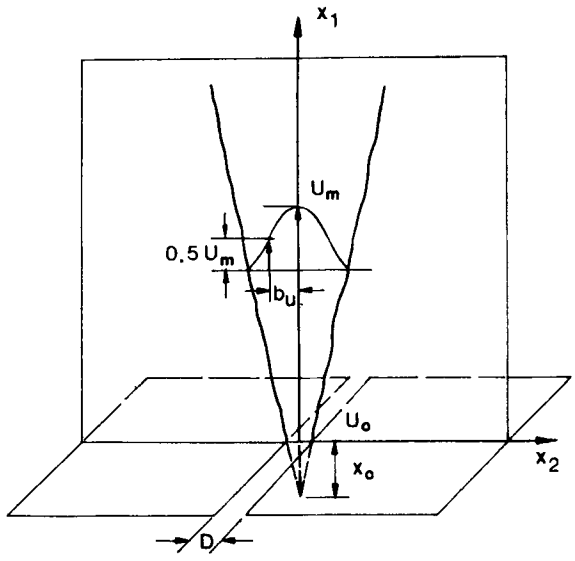

Figure 1. Schematic diagram of a plane vertical jet

For the elliptic solution method adopted, boundary conditions were required on all four sides of the solution domain. The jet centreline was treated as an axis of symmetry. Along the wall the velocity components and the normal gradients of the turbulence kinetic energy and dissipation rate were set equal to zero. At the outer edge of the solution domain the transverse gradient of each velocity component was set equal to zero. Note that for a plane jet, in contradistinction to the axisymmetric case, the entrainment velocity does not go to zero in the far field but assumes a constant value for a given distance downstream of the slot.

The fourth boundary condition pertains to the last downstream plane, where a zero-gradient outflow was imposed. For the streamwise velocity component this was the same as asserting a constant streamwise mass flux for each control volume in the last downstream plane. This is physically unrealistic in a jet flow in two regards. Firstly, the centreline velocity is decaying in the streamwise direction. Secondly, for a rectangular mesh this results in zero entrainment at the exit plane. Comparison of the solution fields, obtained using grids of different streamwise dimension, with each other and also with the similarity behaviour for a plane jet indicated that typically the influence of the outflow boundary condition was limited to a region approximately five slot widths upstream of the outflow plane. In the solution fields considered, care was taken to ensure that the influence of this approximation did not extend into the domain of interest.

Boundary conditions were also required for the velocity components, the turbulence kinetic energy, the dissipation rate and the Reynolds shear stress at the slot. Initially, 'top-hat' profiles were selected with discharge turbulence levels of

$$(k/U_m^2)_0 = 0{\cdot}01, \qquad (\varepsilon D/U_m^3)_0 = 0{\cdot}001.$$

As such the discharge flow from the slot represented a uniform, low-intensity turbulent stream. This initial approach was consistent with the fact that the level of grid resolution required to accurately model the flow field immediately downstream of the slot was beyond the scope of the present study.

In order to assess the influence of the initial conditions at the slot on the developed region of the flow, a second set of profiles was implemented corresponding to the fully developed turbulent channel flow considered in the experimental study of Hussain and Clark.[7] The grid was refined so that eight control volumes were located within the half-slot. The mean velocity profile corresponded to the experimental profile for flow C125. Since profiles for k, ε and $\langle u_1 v_2 \rangle$ were not available from the original study, these values were approximated by curves typical of a fully developed turbulent channel flow. The review of Patel *et al.*[14] identifies typical near-wall behaviour for these parameters. As will be documented in Section 4, the specific initial conditions significantly affected the development region just downstream of the slot.

The computational model used in the study involved numerous approximations. In order to demonstrate an acceptable level of grid independence, the velocity field was calculated on a number of different grids of different sizes and mesh densities. For a specific grid the size of the control volumes was varied to concentrate control volumes along the centreline and just downstream of the slot. In the present study attention was focused on the region 20–40 slot widths downstream of the discharge plane, for which pressure measurements were available. Within this region the prediction for the mean pressure field on different grids was compared in terms of the centreline pressure and the transverse pressure profile at $x_1/D = 25$. Two different grids were used for the final comparison, representing a variation in mesh density of approximately 100%. The maximum variation in mean pressure on these two grids was less than 3%.

The calculations presented below pertain to a rectangular grid extending approximately 60 slot widths in the streamwise direction and 21·5 slot widths in the transverse direction. The grid used 85 and 53 control volumes in the streamwise and transverse directions respectively, with

eight control volumes placed within the half-slot at the discharge plane. On the basis of the grid refinement analysis presented above, the solution was considered to be within a few per cent of truly grid-independent values. This variation was much less than the estimated error in the experimental data available for comparison.

4. RESULTS

The computational model was used to predict the solution field for a plane isothermal turbulent jet with a Reynolds number $Re = U_0 D/\nu = 81\,400$ based on the exit centreline velocity U_0 and slot width D. The numerical results for the mean pressure field are compared with the experimental data of Hussain and Clark,[7] specifically flow C125, corresponding to a plane air jet, also with a Reynolds number of 81 400. The initial velocity profile in the experiment closely resembled a fully developed turbulent channel flow. Unless stated otherwise, all the numerical results presented below are also based on an initial velocity profile which closely resembled a turbulent channel flow.

To begin, consider the prediction for the mean velocity field. Chen and Rodi[15] show that in the similarity region of a plane jet the decay rate of the centreline velocity U_m is given by

$$U_m/U_0 = A_u(x_1/D)^{-1/2} \tag{9}$$

and the velocity half-width b_u grows linearly in the streamwise direction, i.e.

$$S_u = \mathrm{d}b_u/\mathrm{d}x_1 = \text{constant}. \tag{10}$$

Both of these similarity relations are derived using the boundary layer form of the mean transport equations. The predicted values of the similarity parameters, $A_u = 2{\cdot}2$ and $S_u = 0{\cdot}12$, compare favourably with the recommended values $A_u = 2{\cdot}4$ and $S_u = 0{\cdot}11$ of Chen and Rodi.[15]

The development of the turbulence field is presented in Figure 2 in terms of the centreline turbulence intensity. Also shown is a smooth curve fitted to the data of Hussain and Clark.[7] Both the numerical and experimental flow fields are characterized by a sharp rise in the centreline turbulence intensity within the first 20 slot widths and a very gradual increase to the similarity level thereafter.

Also shown is the centreline turbulence intensity for the solution field obtained assuming uniform profiles for U_1, k and ε at the slot. Note that in the region just downstream of the slot the level of turbulence intensity is initially much higher and the development of the turbulence field significantly different. However, all three curves approach the same level for u_1/U_m along the centreline far downstream of the slot. Not surprisingly, the mean velocity field based on uniform profiles at the slot was also characterized by a rate of development more rapid than that of the experimental field.

In the present study attention was focused on the region 20–40 slot widths downstream of the slot. For this region of the flow the distribution of the pressure field, referenced to the value of the ambient pressure at the discharge plane, is presented graphically in Figure 3 as viewed from the jet centreline. The pressure field forms a valley or 'trough' between the centreline and edge of the jet. Over most of the jet the pressure field is negative in value. The trough becomes both broader and shallower as the flow develops in the streamwise direction. The ambient pressure at the edge of the jet is seen to be almost uniform, even though the flow in this region is not zero.

The mean pressure along the jet centreline, normalized using the discharge velocity U_0, is presented in Figure 4. Also shown for comparison is a smooth curve fit to the experimental data of Hussain and Clark.[7] Both distributions have similar shapes; however, the magnitude of the experimental curve is greater than that of the predicted curve. Both curves also indicate a small

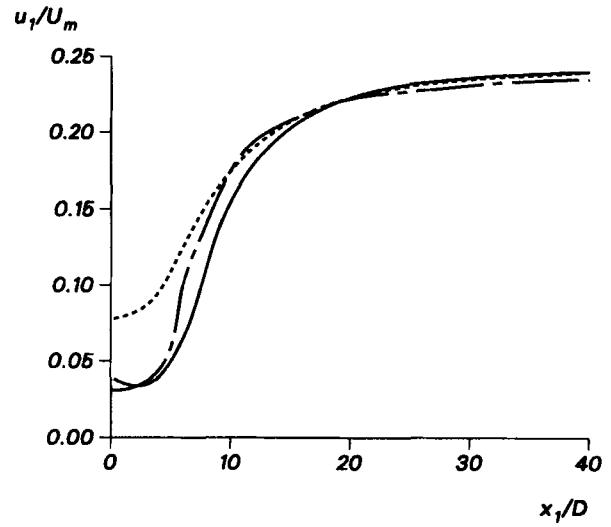

Figure 2. Streamwise turbulence intensity along the centreline of a plane jet: — - —, data;[7] ——, ASM with channel profile; - - - -, ASM with uniform profile

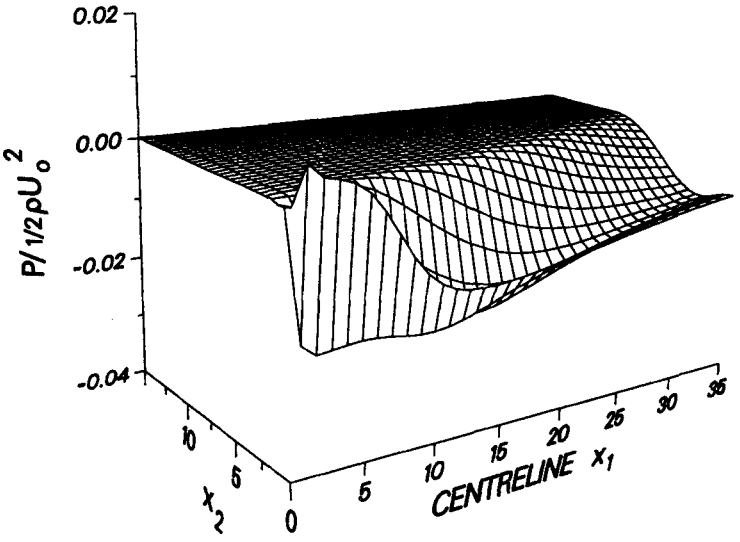

Figure 3. ASM prediction of the mean pressure field in a plane jet

region of positive pressure just downstream of the slot. A positive pressure was also measured at the slot exit plane by Quinn and Militzer[8] in their study of a turbulent free square jet. Although the prediction of a positive pressure in this region appears to be realistic, the sensitivity of the flow field to the level of grid refinement and specific turbulence conditions at the slot precludes further comment.

Figure 5 plots the mean pressure profiles along consecutive transverse sections. In each case the mean pressure is normalized using the local value of the jet centreline velocity U_m. From

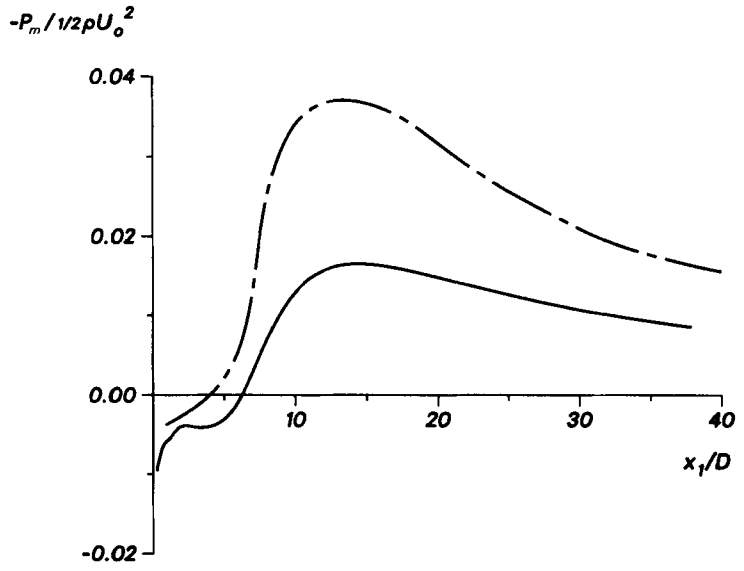

Figure 4. Mean pressure along the centreline of a plane jet: — – —, data;[7] ——, ASM

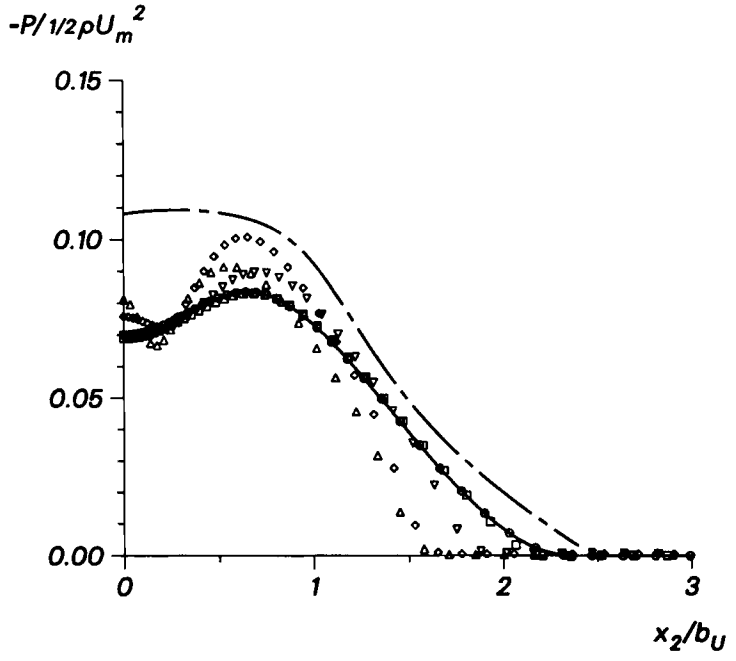

Figure 5. Profiles of the mean pressure in a plane jet: — – —, data;[7] △, ◇, ▽, □, ⊖, ASM at $x_1/D = 20, 25, 30, 35, 40$ respectively

Figure 5 one can conclude that the pressure profile for the predicted velocity field becomes self-similar within approximately 35 slot widths of the discharge plane. Also shown in Figure 5 is a smooth curve fitted to the experimental profile of Hussain and Clark.[7] Their results suggest that self-similar behaviour was obtained by approximately $x_1/D=20$. Again the magnitude of the experimental profile is noticeably greater than the predicted value, especially in the region close to the jet centreline. Hussain and Clark[7] acknowledged some uncertainty in their static pressure measurements due to the undetermined influence of turbulence.

The magnitude of the mean pressure field is closely related to the level of the the transverse normal Reynolds stress component $\langle u_2 u_2 \rangle$. Hussain and Clark[7] show that for the similarity region where streamwise gradients can be neglected, integration of the transverse momentum equation between the edge of the jet and an internal point within the jet results in the following expression for the pressure:

$$P - P_e = -\rho \langle u_2 u_2 \rangle + (\rho/2)(U_{2e}^2 - U_2^2), \tag{11}$$

where the subscript 'e' denotes variables evaluated at the edge of the flow.

First, consider the contribution of the transverse velocity component in equation (11). Figure 6 plots the transverse velocity component U_2, normalized by the centreline velocity, across the jet. Also shown is the experimental profile of Ramaprian and Chandrasekhara,[2] although they suggest their magnitude for U_2 at the outer edge is somewhat low. The transverse velocity reaches a maximum magnitude at the edge of the jet equal to the so-called entrainment velocity U_{2e}. For a plane jet this value is typically $U_{2e}/U_m = 0{\cdot}06$.[2] While substantially less than the centreline velocity, the entrainment velocity is much larger than the local value of the streamwise velocity component, which goes to zero.

Returning to equation (11), since U_2 is always less than the value U_{2e} at the edge, a negative pressure follows from the positive value of the Reynolds stress component $\langle u_2 u_2 \rangle$. Figure 7 shows the predicted profile for $\langle u_2 u_2 \rangle$ at $x_1/D=40$, together with the experimental profile of Ramaprian and Chandrasekhara.[2] The profile predicted by the algebraic stress model for $\langle u_2 u_2 \rangle$ is greater than the experimental value. This implies that substitution of the experimental profile of Ramaprian and Chandrasekhara[2] into equation (11) would yield even lower values for the

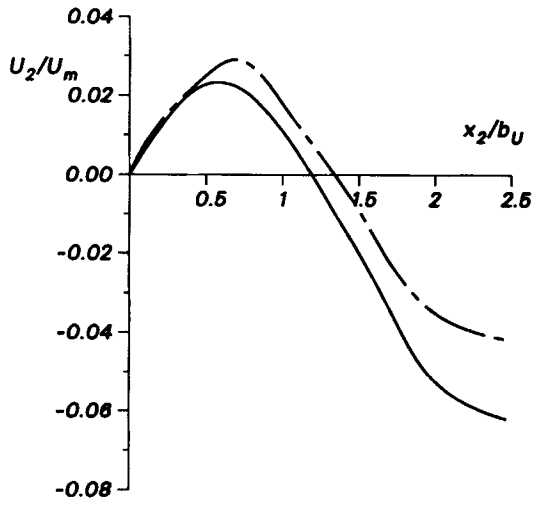

Figure 6. Profile of the transverse component of the mean velocity in a plane jet: — – —, data;[2] ——, ASM

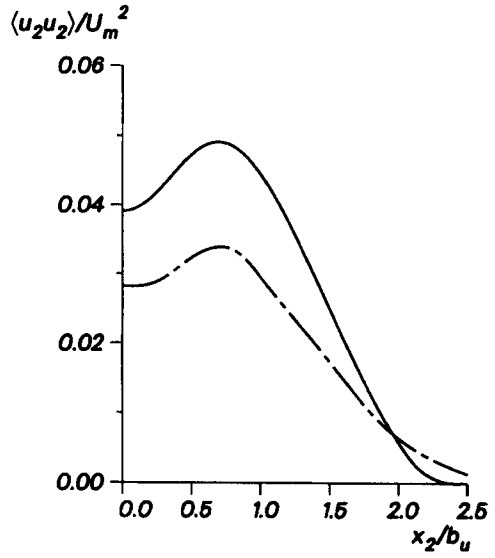

Figure 7. Profile of the transverse normal Reynolds stress component $\langle u_2u_2\rangle$ in a plane jet: — — —, data;[2] ——, ASM

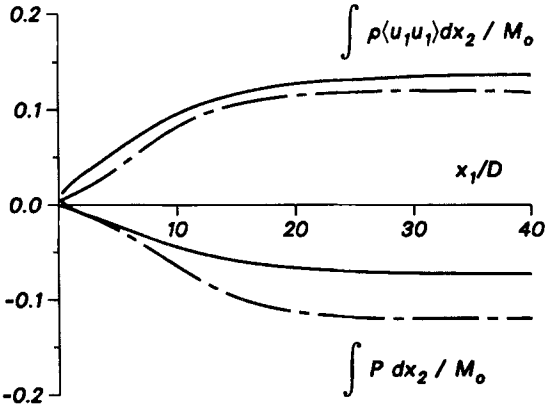

Figure 8. Contribution of the Reynolds stress $\langle u_1u_1\rangle$ and mean pressure P to the balance of streamwise momentum in a plane jet: — — —, data;[7] ——, ASM. $M_0=\rho U_1^2 D$ at the slot

magnitude of the mean pressure profile. Since the predicted magnitude of the pressure profile is already low relative to the measured value, this would seem to indicate some inconsistency between the two experimental studies.

Finally, consider the contribution of the mean pressure field to the overall balance of streamwise momentum in the jet. Integration of the streamwise momentum equation across the width of the jet yields the following relation:

$$\int_{-\infty}^{\infty} (\rho U_1^2 + \rho\langle u_1u_1\rangle + P)\, dx_2 = \text{constant}, \tag{12}$$

which asserts conservation of the total jet momentum flux. In addition to the streamwise momentum ρU_1^2, equation (12) also includes contributions from the streamwise Reynolds normal stress component $\rho\langle u_1 u_1\rangle$ and the mean pressure P. As pointed out by Ramaprian and Chandrasekhara,[2] the momentum flux reported by different experimental studies varies significantly, assuming asymptotic values in the far downstream region which are both smaller and larger than the nominal discharge value at the slot.

Figure 8 plots the streamwise variation of the integral of the normal Reynolds stress component $\langle u_1 u_1\rangle$ and the mean pressure P for the jet, together with the experimental results of Hussain and Clark.[7] The contributions of $\langle u_1 u_1\rangle$ and P are positive and negative respectively and both appear to reach constant asymptotic values beyond $x_1/D=25$. The numerical results presented in Figure 8 imply that the contribution of ρU_1^2 to the total momentum flux in equation (12) decreases to an asymptotic value of approximately 95% of the initial value $\rho U_1^2 D$ at the slot. The magnitude of the contribution of the pressure field to the integral in equation (12) is approximately 7%, that of the normal Reynolds stress approximately 14%.

5. CONCLUSIONS

The present study considered a numerical prediction for the mean pressure field in a plane turbulent jet. The mean momentum equation was closed using an algebraic stress model relation for the Reynolds stress tensor. The full two-dimensional form of the transport equation set was retained and solved elliptically.

The numerical prediction for the pressure field was compared with the experimental data of Hussain and Clark.[7] The predicted and experimental fields were generally similar; however, the overall level predicted for the pressure field was lower than that of the measurements. This discrepancy suggests a deficiency in the algebraic stress model for the Reynolds stress $\langle u_2 u_2\rangle$, a systematic error in the pressure measurements or perhaps both. In any event further measurements of the pressure field in a plane turbulent jet are required to resolve this question.

With respect to the conservation of mean streamwise momentum in the jet, the contribution of the pressure field is negative and opposes that of the streamwise Reynolds stress component $\langle u_1 u_1\rangle$. The contribution of the mean velocity term U_1^2 decreases in the streamwise direction to an asymptotic value which is approximately 95% of the value at the slot. As such, pressure has a relatively small effect on the streamwise momentum balance.

The present study only briefly considered the flow field in the region immediately downstream of the slot. A more in-depth study would require not only a much finer computational grid but also documentation of the initial conditions upstream of the discharge plane. However, once additional experimental data become available, this flow region would represent an interesting test of the performance of an algebraic stress model in a rapidly developing turbulent shear flow.

ACKNOWLEDGEMENT

This research was funded by the Natural Sciences and Engineering Research Council of Canada.

REFERENCES

1. F. M. White, *Viscous Fluid Flow*, McGraw-Hill, New York, 1974.
2. B. R. Ramaprian and M. S. Chandrasekhara, 'LDA measurements in plane turbulent jets', *ASME J. Fluids Eng.*, **107**, 264–271 (1985).
3. F. C. Gouldin, R. W. Schefer, S. C. Johnson and W. Kollman, 'Nonreacting turbulent mixing flows', *Prog. Energy Combust. Sci.*, **12**, 257–303 (1986).

4. M. S. Hossain and W. Rodi, 'A turbulence model for buoyant flows and its application to vertical buoyant jets', in W. Rodi (ed.), *Turbulent Buoyant Jets and Plumes, HMT, Vol. 6*, Pergamon, New York, 1982, pp. 121–178.
5. D. R. Miller and E. W. Comings, 'Static pressure distribution in a free turbulent jet', *J. Fluid Mech.*, **3**, 1–16 (1957).
6. L. J. S. Bradbury, 'The structure of a self-preserving turbulent plane jet', *J. Fluid Mech.*, **23**, 31–64 (1965).
7. A. K. M. F. Hussain and A. R. Clark, 'Upstream influence on the near field of a plane turbulent jet', *Phys. Fluids*, **20**, 1416–1426 (1977).
8. W. R. Quinn and J. Militzer, 'Experimental and numerical study of a turbulent free square jet', *Phys. Fluids*, **31**, 1017–1025 (1988).
9. M. M. Gibson and B. E. Launder, 'On the calculation of horizontal non-equilibrium turbulent shear flows under gravitational influence', *J. Heat Transfer, ASME*, **98**, 81–87 (1976).
10. J. F. Sini and I. Dekeyser, 'Numerical prediction of turbulent plane jets and forced plumes by use of the k–ε model of turbulence', *Int. J. Heat Mass Transfer*, **30**, 1787–1801 (1987).
11. V. Haroutunian and B. E. Launder, 'Second-moment modelling of free buoyant shear flows: a comparison of parabolic and elliptic solutions', in J. S. Puttock (ed.), *Stably Stratified Flow and Dense Gas Dispersion*, Oxford University Press, Oxford, 1988, pp. 409–430.
12. G. D. Raithby, P. F. Galpin and J. P. Van Doormaal, 'Prediction of heat and fluid flow in complex geometries using general orthogonal coordinates', *Numer. Heat Transfer*, **9**, 125–142 (1986).
13. D. J. Bergstrom, G. D. Stubley and A. B. Strong, 'A computational structure for second order algebraic turbulence models', *Proc. 5th Int. Conf. on Numerical Methods in Laminar and Turbulent Flow*, Pineridge, Swansea, 1987, pp. 1503–1514.
14. V. C. Patel, W. Rodi and G. Scheuerer, 'Turbulence models for near-wall and low Reynolds number flows: a review', *AIAA J.*, **23**, 1308–1319 (1988).
15. C. J. Chen and W. Rodi, *Turbulent Buoyant Jets—A Review of Experimental Data, HMT, Vol. 4*, Pergamon, Oxford, 1980.